Int. J. Heat Mass Transfer. Vol. 33, No. 1, pp. 127–138, 1990
Printed in Great Britain

0017–9310/90 $3.00 + 0.00

Thermal protection from intense localized moving heat fluxes using phase-change materials

YIDING CAO and AMIR FAGHRI
Department of Mechanical Systems Engineering, Wright State University, Dayton, OH 45435, U.S.A.

(*Received* 18 *October* 1988 *and in final form* 27 *April* 1989)

Abstract—Various technologies which protect a wall from being burned out by an intense localized moving heat source have been reviewed, and a solution to this problem is proposed in which a phase-change material (PCM) is placed underneath the wall to absorb the high heat flux. The three-dimensional melting problem is nondimensionalized and modeled with a new enthalpy transforming scheme. The numerical results show that the proposed solution reduces the peak wall temperature significantly. The method of coating the PCM on the wall surface is also employed, which can maintain the surface temperature below the melting temperature of the PCM.

INTRODUCTION

HEAT TRANSFER in a body resulting from a moving heat source is a well-known heat transfer problem and has broad applications in the fields of welding, laser and electron beam surface processing, etc. In these cases, a surface is subjected to a localized heat input, and the incoming heat flux moves relative to the surface. The interest in the above applications is how to heat the surface effectively. However, in some applications a surface is hit by a moving high intensity heat source, as shown in Fig. 1. The major concern here is how to protect the surface from being burned out by the moving heat flux. This is indeed a problem of concern in laser thermal threats and re-entry situations and has been one of the motivations of the present study.

The methods used to protect surfaces from being burned out by a high heat flux are usually ablation and heat pipe technologies. Most of the previous studies on ablation concentrated on a stationary heat input with a large heating area. The major concern for this problem is the total energy which must be absorbed during a given time period. In the ablation technology which is used in missile re-entry situations, the surface of the body is coated with a solid material which is exposed to the high heat flux and is allowed to melt and blow away. Thus, a large amount of the incoming heat is expended in melting the material rather than being conducted into the interior of the vehicle, so that the temperature of the vehicle surface is reduced. The thickness of the coated material must be greater than the melted thickness during this time period. The drawback of this technology is that once the coated material has melted, it is immediately blown away. The coated surface can be used only once, and for the next mission one must coat the surface again. For vehicles which have frequent missions such as airplanes, this situation may be intolerable. Moreover, high speed vehicles require a smooth surface to reduce the flow resistance and to reject the incoming heat; coated or ablated surfaces may have difficulties in reaching this goal. Nevertheless, due to the simplicity and effectiveness of this method, it still remains an alternative to protecting the surface and may be adopted to the case of a moving heat source.

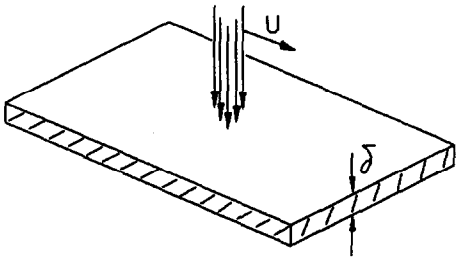

FIG. 1. A wall surface subject to an intense localized moving heat source.

Heat pipe technology is a good means of protecting a surface from attack by a high heat flux. For the present moving heat source problem, however, the heat pipe may only work under melting or free molecular conditions. Furthermore, a heat pipe is an integral vessel which cannot allow vapor leakage, which means that the present manufacturing technology would not be easily adapted to vehicles that have a large surface area. For these reasons, the adoption of heat pipe technology for the present problem is not economical.

Recently, the study of phase-change materials is active due to applications to space-based power plants and the utilization of solar energy. Phase-change materials (PCMs) have a large melting heat, so it is an efficient way to absorb the heat energy during the time period when the materials are subjected to heat input and to release it afterward at a relatively constant temperature. It is advantageous to incorporate

NOMENCLATURE

a	coefficient
b	source term in the discretization equation
C	specific heat per unit volume [J m^{-3} K^{-1}]
C_{lw}	dimensionless number, C_l/C_w
C_{sw}	dimensionless number, C_s/C_w
c	specific heat [J kg^{-1} K^{-1}]
E	enthalpy [J kg^{-1}]
F	flow rate through a control-volume face [kg s^{-1}]
H	latent heat [J kg^{-1}]
h	total thickness, $\delta_p+\delta$
h^*	dimensionless number, h/R_h
k	thermal conductivity [W m^{-1} K^{-1}]
K_{lw}	dimensionless number, k_l/k_w
K_{sw}	dimensionless number, k_s/k_w
n	normal outward direction
n^*	dimensionless normal outward direction, n/R_h
N_t	dimensionless number, $T_i/(T_m-T_i)$
N_v	dimensionless number, $UC_w(T_m-T_i)/q_h$
N_Q	dimensionless number, $q_hR_h/(T_m-T_i)k_w$
N_r	dimensionless number, $R_h(T_m-T_i)^3\sigma\varepsilon/k_w$
Q	heat source power [W]
q_h	heat flux [W m^{-2}]
R_h	heat source radius [m]
R_0	radius of the numerical domain [m]
r	radial coordinate
St	Stefan number, $c_s(T_m-T_i)/H$
S	coefficient in equation (19)
T_i	initial temperature [K]
T_m	melting temperature [K]
T^*	dimensionless temperature, $(T-T_i)/(T_m-T_i)$
T^+	'Kirchhoff' temperature defined in equation (17)
t	time [s]
Δt	time step
t^*	dimensionless number, $tk_w/(C_wR_h^2)$
U	heat source velocity [m s^{-1}]
U^*	dimensionless velocity, C_wUR_h/k_w
v_n	normal melting/freezing speed [m s^{-1}]
ΔV	volume of the control volume [m^3]
u, v, w	velocities [m s^{-1}]
x, y, z	moving coordinate directions
x', y', z'	fixed coordinate directions
x^*, y^*, z^*	dimensionless distances, x/R_h, y/R_h, z/R_h
X–X	plane indicated in Figs. 4 and 14.

Greek symbols

α	thermal diffusivity [m^2 s^{-1}]
Γ	coefficient in equation (19)
δ	wall thickness [m]
δ^*	dimensionless wall thickness, δ/R_h
δ_m	maximum melting front depth [m]
δ_m^*	dimensionless maximum melting front depth, δ_m/R_h
δ_p	thickness of the PCM [m]
δ_p^*	dimensionless thickness of the PCM, δ_p/R_h
ε	emissivity
η	dummy variable in equation (17)
θ	tangential coordinate
ρ	density [kg m^{-3}]
σ	Stefan–Boltzmann constant [W m^{-2} K^{-4}].

Subscripts

B	'bottom' neighbor of grid P
b	control-volume face between P and B
E	'east' neighbor of grid P
e	control-volume face between P and E
i	initial condition
l	liquid phase
m	mushy phase
N	'north' neighbor of grid P
n	control-volume face between P and N or normal outward direction
P	grid point
S	'south' neighbor of grid P
s	control-volume face between P and S or solid phase
T	'top' neighbor of grid P
t	control-volume face between P and T
W	'west' neighbor of grid P
w	control-volume face between P and W or wall.

the merits of the above technologies and propose another alternative to protect the surface from attack by a high heat flux for the present problem, as shown in Fig. 2. There, the incoming heat input moves along the surface with speed U and the heat is conducted through the outside wall to the PCM. The PCM beneath the surface melts and absorbs a large amount of the incoming heat. Because of the large melting latent heat of the PCM and the constant melting temperature T_m, the peak wall temperature will be maintained at a temperature moderately higher than T_m. With a low or moderate T_m, the reduction of the peak wall temperature is evident. The dividing sheet, the soft insulating material and the supporting plate may be used to prevent the separation of the PCM from the surface wall during the melting process, and to prevent the incoming heat from being conducted into the cabin. Because the density of liquid PCM is different from that of solid PCM, there is a tendency for the solid PCM to separate from the outside wall, or

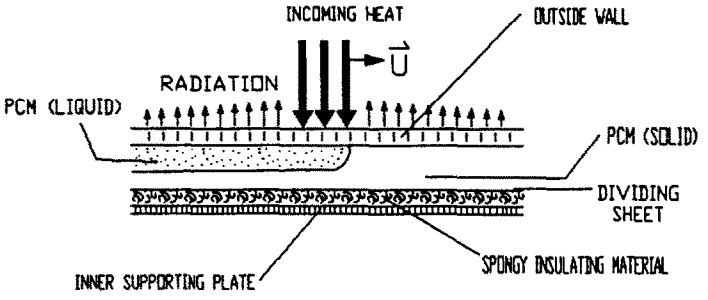

FIG. 2. Configuration to protect surfaces from attack by high heat fluxes.

to form voids near the wall, which reduces the heat transfer into the PCM. If the thickness of the PCM is thin and the density difference is not large, this situation will not be very severe.

The method proposed above imposes few difficulties on the present manufacturing technology, and might also be used as a means of cooling the leading edges of space vehicles in re-entry situations. Since the re-entry time is short, a moderate thickness of the PCM will greatly reduce the temperature jump at the leading edges.

A numerical analysis of the problem mentioned above is given in this paper and the important parameters in protecting surfaces from an intense localized moving heat flux using PCM are identified and discussed.

ANALYSIS OF PHASE CHANGE WITH A MOVING HEAT SOURCE

The present problem mentioned above is a three-dimensional phase-change problem with a moving heat source. Since the focus here is on space applications and the PCM thickness is comparatively thin, the natural convection due to gravity will not be considered. Also, since the layer of the PCM is thin, the influence of the density change between the solid and the liquid phases is expected to be small, and will be ignored.

In a Cartesian coordinate system (x', y', z') fixed at the outside wall as shown in Fig. 3, the heat source moves relative to the plate with speed U on the surface. The appropriate energy equation is [1]

$$\rho\frac{\partial E}{\partial t}=\frac{\partial}{\partial x'}\left(k\frac{\partial T}{\partial x'}\right)+\frac{\partial}{\partial y'}\left(k\frac{\partial T}{\partial y'}\right)+\frac{\partial}{\partial z'}\left(k\frac{\partial T}{\partial z'}\right) \quad (1)$$

where the relation between E and T is given by the equation of state, $dE/dT = c$. This equation is applicable to the three different regions, namely, the wall, the solid PCM, and the liquid PCM with different relations between the enthalpy E, and temperature T, and the appropriate physical properties.

An analysis in a fixed coordinate system is difficult for this problem. It is convenient to study it in a moving coordinate system where the origin is fixed at the heated spot. Imagine an observer riding along with the incoming heat beam. The outside wall and the PCM will travel by at the same speed $-U$. If we fix a moving coordinate system (x, y, z) to the center of the beam, the system will appear in reference to the fixed coordinate system as shown in Fig. 3.

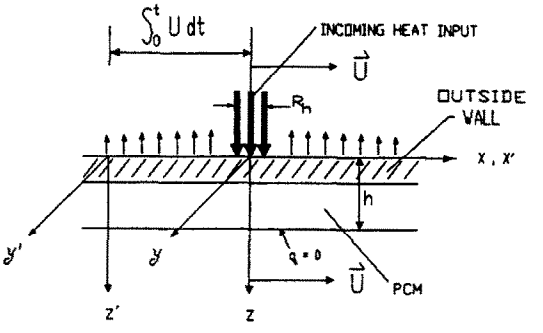

FIG. 3. Description of different coordinate systems and their relationships.

In the moving coordinate system, the problem becomes a convective and diffusive heat transfer problem. The governing equation according to Kays and Crawford [1] is

$$\rho\frac{DE}{Dt}=\frac{\partial}{\partial x}\left(k\frac{\partial T}{\partial x}\right)+\frac{\partial}{\partial y}\left(k\frac{\partial T}{\partial y}\right)+\frac{\partial}{\partial z}\left(k\frac{\partial T}{\partial z}\right). \quad (2)$$

With $u = -U$, $v = w = 0$, we have

$$\rho\frac{DE}{Dt}=\rho\frac{\partial E}{\partial t}-\rho U\frac{\partial E}{\partial x}. \quad (3)$$

Equation (2) then becomes

$$\rho\frac{\partial E}{\partial t}-\rho U\frac{\partial E}{\partial x}=\frac{\partial}{\partial x}\left(k\frac{\partial T}{\partial x}\right)+\frac{\partial}{\partial y}\left(k\frac{\partial T}{\partial y}\right)+\frac{\partial}{\partial z}\left(k\frac{\partial T}{\partial z}\right). \quad (4)$$

The second term on the left-hand side of the equation is a convective term, while the terms on the right-hand side are diffusive terms.

The relations between the variables of the two co-

ordinate systems are evident, i.e. $y = y'$, $z = z'$ and

$$x = x' - \int_0^t U \, dt.$$

When U is a constant, $x = x' - Ut$.

In the case of constant physical properties for the wall, the solid PCM and the liquid PCM, the phase change occurs at a single temperature. Equation (4) can be written for each region as

$$\frac{C_w}{k_w}\frac{\partial T}{\partial t} - \frac{C_w}{k_w}U\frac{\partial T}{\partial x} = \frac{\partial^2 T}{\partial x^2} + \frac{\partial^2 T}{\partial y^2} + \frac{\partial^2 T}{\partial z^2} \quad \text{(wall)}$$

$$\frac{C_s}{k_s}\frac{\partial T}{\partial t} - \frac{C_s}{k_s}U\frac{\partial T}{\partial x} = \frac{\partial^2 T}{\partial x^2} + \frac{\partial^2 T}{\partial y^2} + \frac{\partial^2 T}{\partial z^2} \quad \text{(solid PCM)}$$

$$\frac{C_l}{k_l}\frac{\partial T}{\partial t} - \frac{C_l}{k_l}U\frac{\partial T}{\partial x} = \frac{\partial^2 T}{\partial x^2} + \frac{\partial^2 T}{\partial y^2} + \frac{\partial^2 T}{\partial z^2} \quad \text{(liquid PCM)} \quad (5)$$

where $C_w = c_w\rho_w$, $C_s = c_s\rho_s$ and $C_l = c_l\rho_l$. The initial and boundary conditions are

$t = 0$:

$$T = T_i, \quad 0 \leqslant z < h, \quad -\infty < x < \infty, \quad -\infty < y < \infty$$

$t > 0$:

$$k_w\frac{\partial T}{\partial z} = q_h, \quad z = 0, \quad \sqrt{(x^2+y^2)} \leqslant R_h$$

$$k_w\frac{\partial T}{\partial z} = \sigma\varepsilon T^4, \quad z = 0, \quad \sqrt{(x^2+y^2)} > R_h$$

$$q|_{\delta_-} = q|_{\delta_+}, \quad z = \delta, \quad -\infty < x < \infty, \quad -\infty < y < \infty$$

$$\frac{\partial T}{\partial z} = 0, \quad z = h, \quad -\infty < x < \infty, \quad -\infty < y < \infty$$

$$T = T_i, \quad 0 \leqslant z \leqslant h, \quad |x| \to \infty, \quad |y| \to \infty$$

$$u = U, \quad w = v = 0, \quad 0 \leqslant z \leqslant h$$

$$-\infty < x < \infty, \quad -\infty < y < \infty. \quad (6)$$

At the liquid and solid interface within the PCM, we have

$$T_s = T_l = T_m$$

$$-k_l\frac{\partial T_l}{\partial n} + k_s\frac{\partial T_s}{\partial n} = Hv_n\rho. \quad (7)$$

To reduce the number of parameters that have to be specified for the numerical solutions, the following dimensionless variables are introduced:

$$x^* = \frac{x}{R_h}, \quad y^* = \frac{y}{R_h}, \quad z^* = \frac{z}{R_h}, \quad T^* = \frac{T-T_i}{T_m-T_i}$$

$$U^* = \frac{C_w U}{k_w}R_h, \quad t^* = \frac{k_w t}{C_w R_h^2}. \quad (8)$$

Equations (5)–(7) are nondimensionalized as

$$\frac{\partial T^*}{\partial t^*} - U^*\frac{\partial T^*}{\partial x^*} = \frac{\partial^2 T^*}{\partial x^{*2}} + \frac{\partial^2 T^*}{\partial y^{*2}} + \frac{\partial^2 T^*}{\partial z^{*2}} \quad \text{(wall)}$$

$$\frac{C_s}{C_w}\frac{k_w}{k_s}\frac{\partial T^*}{\partial t^*} - \frac{C_s}{C_w}\frac{k_w}{k_s}U^*\frac{\partial T^*}{\partial x^*} = \frac{\partial^2 T^*}{\partial x^{*2}} + \frac{\partial^2 T^*}{\partial y^{*2}} + \frac{\partial^2 T^*}{\partial z^{*2}} \quad \text{(solid PCM)}$$

$$\frac{C_l}{C_w}\frac{k_w}{k_l}\frac{\partial T^*}{\partial t^*} - \frac{C_l}{C_w}\frac{k_w}{k_l}U^*\frac{\partial T^*}{\partial x^*} = \frac{\partial^2 T^*}{\partial x^{*2}} + \frac{\partial^2 T^*}{\partial y^{*2}} + \frac{\partial^2 T^*}{\partial z^{*2}} \quad \text{(liquid PCM)} \quad (9)$$

$t^* = 0$:

$$T^* = 0, \quad 0 \leqslant z^* \leqslant h^*$$

$$-\infty < x^* < \infty, \quad -\infty < y^* < \infty$$

$t^* > 0$:

$$-\frac{\partial T^*}{\partial z^*} = \frac{q_h R_h}{(T_m-T_i)k_w}, \quad z^* = 0, \quad \sqrt{(x^{*2}+y^{*2})} \leqslant 1$$

$$\frac{\partial T^*}{\partial z^*} = \frac{R_h(T_m-T_i)^3\sigma\varepsilon}{k_w}\left(T^* + \frac{T_i}{T_m-T_i}\right)^4$$

$$z^* = 0, \quad \sqrt{(x^{*2}+y^{*2})} > 1$$

$$q|_{\delta_-^*} = q|_{\delta_+^*}, \quad z^* = \delta^* = \frac{\delta}{R_h}$$

$$-\infty < x^* < \infty, \quad -\infty < y^* < \infty$$

$$\frac{\partial T^*}{\partial z^*} = 0, \quad z^* = h^* = \frac{h}{R_h}$$

$$-\infty < x^* < \infty, \quad -\infty < y^* < \infty$$

$$T^* = 0, \quad 0 \leqslant z^* \leqslant h^*, \quad |x^*| \to \infty, \quad |y^*| \to \infty$$

$$u^* = U^*, \quad v^* = w^* = 0, \quad 0 \leqslant z^* \leqslant h^*$$

$$-\infty < x^* < \infty, \quad -\infty < y^* < \infty. \quad (10)$$

At the interface of the liquid and solid in the PCM

$$T_s^* = T_l^* = 1$$

$$\frac{c_s(T_m-T_i)}{H}\left(-\frac{k_l}{k_w}\frac{\partial T_l^*}{\partial n^*} + \frac{k_s}{k_w}\frac{\partial T_s^*}{\partial n^*}\right) = \frac{C_s R_h}{k_w}v_n. \quad (11)$$

The independent dimensionless parameters in addition to those in equation (8) above are

$$\frac{C_s}{C_w}, \frac{C_l}{C_w}, \frac{k_s}{k_w}, \frac{k_l}{k_w}, \quad \frac{q_h R_h}{(T_m-T_i)k_w}$$

$$\delta^*, h^*, \frac{R_h(T_m-T_i)^3}{k_w}\sigma\varepsilon, \quad \frac{T_i}{T_m-T_i}, \quad \frac{c_s(T_m-T_i)}{H}.$$

Upon combining $C_w U R_h/k_w$ with $q_h R_h/(T_m-T_i)k_w$, we get a new dimensionless parameter $UC_w(T_m-T_i)/q_h$ which may be used to replace the dimensionless number $C_w U R_h/k_w$. Also, since $h^* = \delta^* + \delta_p^*$, the independent variable h^* may be replaced by δ_p^*.

Thus, we have

$$T^* = f(N_v, N_Q, St, t^*, N_r, N_t, C_{sw}, C_{lw}, K_{lw}, K_{sw}, \delta^*, \delta_p^*, x^*, y^*, z^*) \quad (12)$$

where

$$T^* = (T-T_i)/(T_m-T_i)$$
$$N_v = UC_w(T_m-T_i)/q_h$$
$$N_Q = q_h R_h/(T_m-T_i)k_w$$
$$St = c_s(T_m-T_i)/H$$
$$t^* = k_w t/(C_w R_h^2)$$
$$N_r = R_h(T_m-T_i)^3\sigma\varepsilon/k_w$$
$$N_t = T_i/(T_m-T_i)$$
$$C_{sw} = C_s/C_w$$
$$C_{lw} = C_l/C_w$$
$$K_{sw} = k_s/k_w$$
$$K_{lw} = k_l/k_w$$
$$\delta^* = \delta/R_h$$
$$\delta_p^* = \delta_p/R_h$$
$$x^* = x/R_h$$
$$y^* = y/R_h$$
$$z^* = z/R_h.$$

NUMERICAL MODEL AND SOLUTION PROCEDURE

The above problem is nonlinear due to the moving front, so that exact analytical solutions for this type of non-linear problem are available only for some simplified and idealized systems. Numerical methods appear to be the only practical approach for handling this three-dimensional melting problem with a moving heat source.

The numerical methods used to solve phase-change problems might be divided into two main groups. The first group is called strong numerical solutions; examples are given by Okada [2], and Ho and Chen [3]. These methods are only applicable to processes involving one or two space dimensions. The second group is called weak numerical solutions [4–7]. These methods allow us to avoid paying explicit attention to the nature of the phase-change front. Recently, a new enthalpy transforming model which starts from equation (4) and transforms the equation into a non-linear equation with a single dependent variable E was proposed [6]. The existing algorithm schemes are flexible and can handle three-dimensional problems without difficulty.

In order to simulate the circular heat source, equation (4) needs to be transformed into the form for the cylindrical coordinate system. Referring to Fig. 4 and

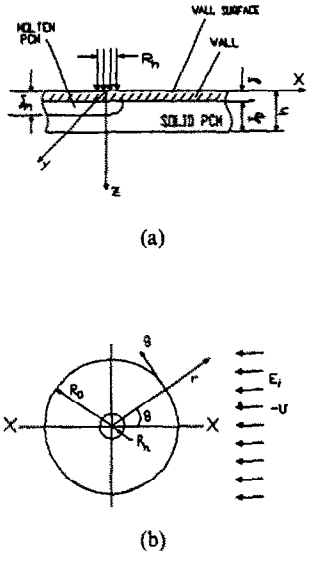

FIG. 4. Pictorial description of the computational domain for the wall–PCM module: (a) side view; (b) top view.

introducing $x = r\cos\theta$, $y = r\sin\theta$, we get

$$\rho\frac{\partial E}{\partial t} + v_r\rho\frac{\partial E}{\partial r} + \rho v_\theta\frac{\partial E}{r\partial\theta} = \frac{1}{r}\frac{\partial}{\partial r}\left(rk\frac{\partial T}{\partial r}\right) + \frac{1}{r}\frac{\partial}{\partial\theta}\left(\frac{k}{r}\frac{\partial T}{\partial\theta}\right) + \frac{\partial}{\partial z}\left(k\frac{\partial T}{\partial z}\right) \quad (13)$$

with

$$v_r = -U\cos\theta, \quad v_\theta = U\sin\theta, \quad v_z = 0.$$

Incorporating the continuity equation

$$\frac{1}{r}\frac{\partial}{\partial r}(r\rho v_r) + \frac{1}{r}\frac{\partial(v_\theta\rho)}{\partial\theta} + \frac{\partial\rho}{\partial t} = 0 \quad (14)$$

we obtain

$$\frac{\partial\rho E}{\partial t} + \frac{1}{r}\frac{\partial(rv_r\rho E)}{\partial r} + \frac{1}{r}\frac{\partial(v_\theta\rho E)}{\partial\theta} = \frac{1}{r}\frac{\partial}{\partial r}\left(rk\frac{\partial T}{\partial r}\right) + \frac{1}{r}\frac{\partial}{\partial\theta}\left(\frac{k\partial T}{r\partial\theta}\right) + \frac{\partial}{\partial z}\left(k\frac{\partial T}{\partial z}\right) \quad (15)$$

with the state equation $dE/dT = c(T)$. Following the analysis given in ref. [6], the transforming method is described as follows.

In the case of constant specific heats for each phase and that the phase change occurs at a single temperature, the relation between temperature and enthalpy can be expressed as follows:

$$T = \begin{cases} T_m + E/c_s, & E \leqslant 0 \quad \text{(solid phase)} \\ T_m, & 0 < E < H \quad \text{(mushy phase)} \\ T_m + (E-H)/c_l, & E \geqslant H \quad \text{(liquid phase).} \end{cases} \quad (16)$$

Here, $E = 0$ has been selected to correspond to phase-change materials in their solid state at temperature T_m.

The 'Kirchhoff' temperature is introduced as

$$T^+ = \int_{T_m}^{T} k(\eta)\,d\eta = \begin{cases} k_s(T-T_m), & T < T_m \\ 0, & T = T_m \\ k_l(T-T_m), & T > T_m. \end{cases} \quad (17)$$

Transforming equation (16) with the definition given in equation (17) results in

$$T^+ = \begin{cases} k_s E/c_s, & E \leqslant 0 \\ 0, & 0 < E < H \\ k_l(E-H)/c_l, & E \geqslant H. \end{cases} \quad (18)$$

An enthalpy function is introduced as follows:

$$T^+ = \Gamma(E)E + S(E). \quad (19)$$

Equation (15) is transformed into a non-linear equation with a single dependent variable E

$$\frac{\partial(E\rho)}{\partial t} + \frac{1}{r}\frac{\partial(rv_r\rho E)}{\partial r} + \frac{1}{r}\frac{\partial(v_\theta \rho E)}{\partial \theta} = \frac{1}{r}\frac{\partial}{\partial r}\left(r\frac{\partial(\Gamma E)}{\partial r}\right) + \frac{1}{r}\frac{\partial}{\partial \theta}\left(\frac{1}{r}\frac{\partial(\Gamma E)}{\partial \theta}\right) + \frac{\partial}{\partial z}\left(\frac{\partial(\Gamma E)}{\partial z}\right) + P \quad (20)$$

where

$$P = \frac{1}{r}\frac{\partial}{\partial r}\left[r\frac{\partial S}{\partial r}\right] + \frac{1}{r}\frac{\partial}{\partial \theta}\left[\frac{1}{r}\frac{\partial S}{\partial \theta}\right] + \frac{\partial^2 S}{\partial z^2}$$

$$v_r = -U\cos\theta, \quad v_\theta = U\sin\theta$$

$$\Gamma = \Gamma(E) = \begin{cases} k_s/c_s, & E \leqslant 0 \\ 0, & 0 < E < H \\ k_l/c_l, & E \geqslant H \end{cases} \quad (21)$$

and

$$S = S(E) = \begin{cases} 0, & E \leqslant 0 \\ 0, & 0 < E < H \\ -Hk_l/c_l, & E \geqslant H. \end{cases} \quad (22)$$

For the wall, no phase change occurs and therefore

$$E = c_w T, \quad \Gamma \equiv k_w/c_w, \quad \text{and} \quad S \equiv 0 \quad (23)$$

with equation (20) still being applicable.

The initial and boundary conditions for the numerical domain in Fig. 4 are as follows:

$t = 0$:

$$E_i = c_w T_i, \quad 0 \leqslant z \leqslant \delta, \quad 0 \leqslant r < \infty, \quad 0 \leqslant \theta \leqslant 360^\circ$$

$$E_i = c_s(T_i - T_m), \quad \delta < z \leqslant h$$

$$0 \leqslant r < \infty, \quad 0 \leqslant \theta \leqslant 360^\circ$$

$t > 0$:

$$-\frac{k_w}{c_w}\frac{\partial E}{\partial z} = q_h, \quad z = 0, \quad r \leqslant R_h, \quad 0 \leqslant \theta \leqslant 360^\circ$$

$$\frac{k_w}{c_w}\frac{\partial E}{\partial z} = \sigma\varepsilon(E/c_w)^4, \quad z = 0, \quad r > R_h, \quad 0 \leqslant \theta \leqslant 360^\circ$$

$$q|_{\delta_+} = q|_{\delta_-}, \quad z = \delta, \quad 0 \leqslant r < \infty, \quad 0 \leqslant \theta \leqslant 360^\circ$$

$$q = 0, \quad z = h, \quad 0 \leqslant r < \infty, \quad 0 \leqslant \theta \leqslant 360^\circ$$

$$E = E_i, \quad 0 \leqslant z \leqslant h, \quad r = R_0, \quad -90^\circ \leqslant \theta \leqslant 90^\circ$$

$$\frac{\partial E}{\partial r} = 0, \quad 0 \leqslant z \leqslant \delta, \quad r = R_0, \quad 90^\circ < \theta < 270^\circ$$

$$\frac{\partial(\Gamma E + S)}{\partial r} = 0, \quad \delta < z \leqslant h$$

$$r = R_0, \quad 90^\circ < \theta < 270^\circ.$$

The radius R_0 must be sufficiently large such that the region $r \geqslant R_0$, $-90^\circ \leqslant \theta \leqslant 90^\circ$ is unaffected by the moving heat source. The last two boundary conditions imply that the upwind scheme is used and the diffusive term is neglected for the outflow boundary.

Equation (20) is discretized with the numerical scheme proposed in ref. [6], which is based on the control-volume finite-difference approach described by Patankar [8]. The general three-dimensional discretization equation for the phase-change problem with a fully implicit scheme in the cylindrical coordinate system is

$$a_P E_P = a_E E_E + a_W E_W + a_N E_N + a_S E_S + a_T E_T + a_B E_B + b \quad (24)$$

where

$$a_P = a_{PE} + a_{PW} + a_{PN} + a_{PS} + a_{PB} + a_{PT} + \frac{\Delta V}{\Delta t}\rho_P^0$$

$$a_E = \Gamma_E D_e + \max[-F_e, 0]$$

$$a_{PE} = \Gamma_P D_e + \max[-F_e, 0]$$

$$a_W = \Gamma_W D_w + \max[F_w, 0]$$

$$a_{PW} = \Gamma_P D_w + \max[F_w, 0]$$

$$a_N = \Gamma_N D_n + \max[-F_n, 0]$$

$$a_{PN} = \Gamma_P D_n + \max[-F_n, 0]$$

$$a_S = \Gamma_S D_s + \max[F_s, 0]$$

$$a_{PS} = \Gamma_P D_s + \max[F_s, 0]$$

$$a_T = \Gamma_T D_t + \max[-F_t, 0]$$

$$a_{PT} = \Gamma_P D_t + \max[-F_t, 0]$$

$$a_B = \Gamma_B D_b + \max[F_b, 0]$$

$$a_{PB} = \Gamma_P D_b + \max[F_b, 0]$$

$$b = \frac{\Delta V \rho_P^0}{\Delta t}E_P^0 + D_e(S_E - S_P) - D_w(S_P - S_W) + D_n(S_N - S_P) - D_s(S_P - S_S) + D_t(S_T - S_P) - D_b(S_P - S_B)$$

where ΔV is the volume of the control volume, $\Delta\theta\,\Delta z(r_n + r_s)/2$, the greater of a and b is given by

$\max[a, b]$, E_P^0 denotes the old value (at time t) of E at grid point P, and ρ_P^0 denotes the old value of ρ at grid point P. The flow rates and conductances are defined as

$$F_e = (\rho v_\theta)_e \Delta r \Delta z, \quad D_e = \frac{\Delta r \Delta z}{r_e(\delta\theta)_e}$$

$$F_w = (\rho v_\theta)_w \Delta r \Delta z, \quad D_w = \frac{\Delta r \Delta z}{r_w(\delta\theta)_w}$$

$$F_n = (\rho v_r)_n \Delta z r_n \Delta\theta, \quad D_n = \frac{\Delta z r_n \Delta\theta}{(\delta r)_n}$$

$$F_s = (\rho v_r)_s \Delta z r_s \Delta\theta, \quad D_s = \frac{\Delta z r_s \Delta\theta}{(\delta r)_s}$$

$$F_t = (\rho v_z)_t r_P \Delta\theta \Delta r, \quad D_t = \frac{r_P \Delta\theta \Delta r}{(\delta z)_t}$$

$$F_b = (\rho v_z)_b r_P \Delta\theta \Delta r, \quad D_b = \frac{r_P \Delta\theta \Delta r}{(\delta z)_b}.$$

Because of the nonlinearity of the above equation and the implicit nature of the scheme, iterations are needed at each time step. This procedure is the same as those which solve a normal non-linear equation.

Since the dimensionless parameters in the last section are independent of the coordinate system, equation (12) is still applicable to the problem in the cylindrical coordinate system of this section.

NUMERICAL RESULTS AND DISCUSSION

The discretization equations above are solved with the Gauss–Seidel method. The grid size employed is $32 \times 30 \times 20$ with the grid size near the wall surface being finer. In order to check the validity of the computer program the calculation has been made with a moving heat source without phase change, i.e. a pure wall without PCM, and the steady-state surface temperature along the X–X plane (the X–X plane corresponds to the plane defined by $\theta = 0°$ and 180° in cylindrical coordinates or $y = 0$ in Cartesian coordinates) was compared with the analytical result of a point source moving on the surface of a semi-infinite medium, as shown in Fig. 5. The steady-state analytical result has the form

$$T - T_i = (Q/2\pi k_w r)\, e^{-(U/2\alpha_w)(r+x)}. \tag{25}$$

The above equation was obtained from a moving Cartesian coordinate system (x, y, z) with the point heat source at the origin and $r = \sqrt{(x^2+y^2+z^2)}$.

The discrepancy between the two results near $x = 0$ is due to the nature of the heat source that was modeled in each case. The analytical result has an infinitesimal heat source at $x = 0$, while the numerical one has a heat source of finite radius R_h. Considering this, the accuracy of the numerical results is very good. The numerical results with radiation ($\varepsilon = 1$) into space for the surface other than the heated spot is also included in Fig. 5. It is shown that the radiation plays no significant role in the temperature distribution of the wall near the heat source, and therefore will not be included in the next discussion, and the radiation parameters N_r and N_t will be dropped.

The general temperature distribution trend on the surface is shown as a three-dimensional plot in Fig. 6. The temperature falls off sharply in the portion of $x^* > 0$, while it falls off gradually for $x^* < 0$. Also, the symmetry of the temperature distribution to the X–X plane indicated in Fig. 4 is evident. Therefore, the representation of the temperature distributions will focus on the X–X plane for simplicity.

(1) *Moving heat source without phase change*

As a first step, a pure wall without PCM is studied. In this situation, equation (12) reduces to

$$T^* = f(N_v, N_Q, t^*, \delta^*, x^*, y^*, z^*). \tag{26}$$

Since the problem is now independent of T_m, $(T_m - T_i)$ is chosen as unity for convenience. Therefore, $T^* = T - T_i$, $N_Q = q_h R_h / k_w$, $N_v = UC_w/q_h$ in this special case.

Figure 7 shows the variation of the steady-state wall

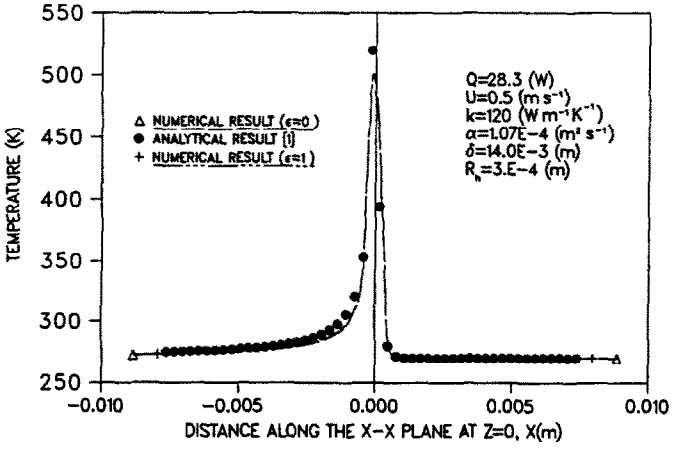

FIG. 5. Comparison between analytical and numerical results without phase change.

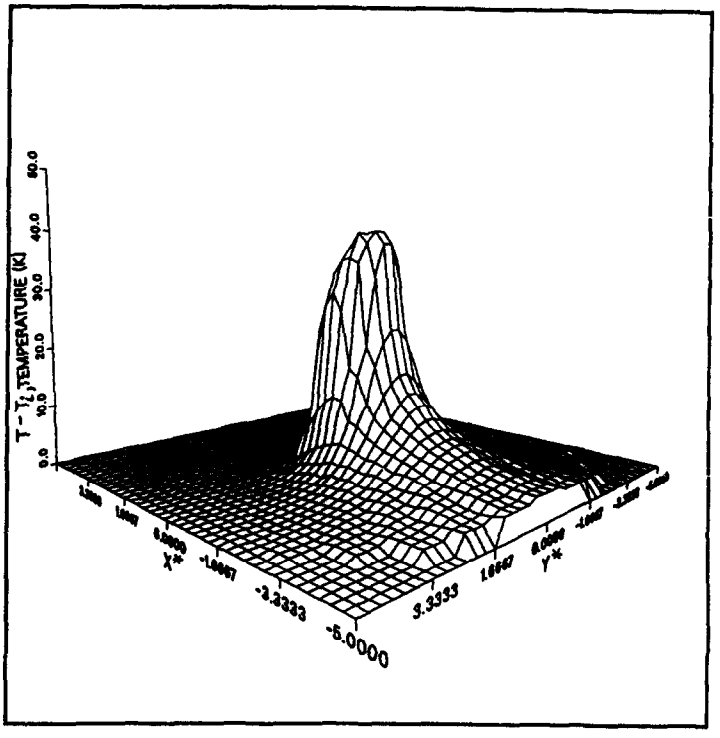

FIG. 6. Graph of the surface temperature distribution trend.

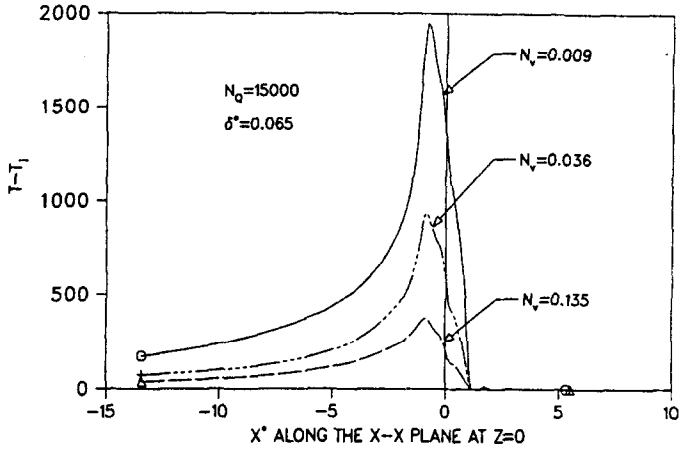

FIG. 7. Steady-state temperature profiles with different N_v without PCM.

surface temperature with different values of N_v. As can be seen, a larger N_v reduces the peak wall temperature significantly, while a small N_v may result in an intolerably high peak wall temperature. The dimensionless number N_Q has an opposite effect on the wall temperature, as shown in Fig. 8. A smaller N_Q corresponds to a lower peak wall temperature, while a larger N_Q corresponds to a higher peak wall temperature. The conclusion can be made that with a certain δ^*, when N_v is large enough or N_Q is small enough, the peak wall temperature is low and the wall does not need to be protected. When N_v is small or N_Q is large, something must be done to protect the wall, otherwise the wall will be burned out. Also, a larger δ^* has the effect of relieving the peak wall temperature, but is often not practical in space applications.

(2) *Moving heat source with PCM underneath the wall*

As mentioned before, one of the alternatives of protecting the wall is to put the PCM beneath the wall as shown in Figs. 2 and 4. Figure 9 shows the numerical isotherms of the dimensionless temperature

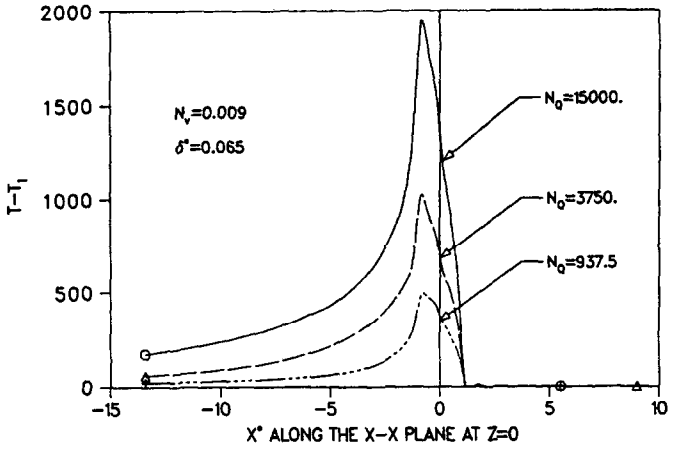

FIG. 8. Steady-state temperature profiles with different N_Q without PCM.

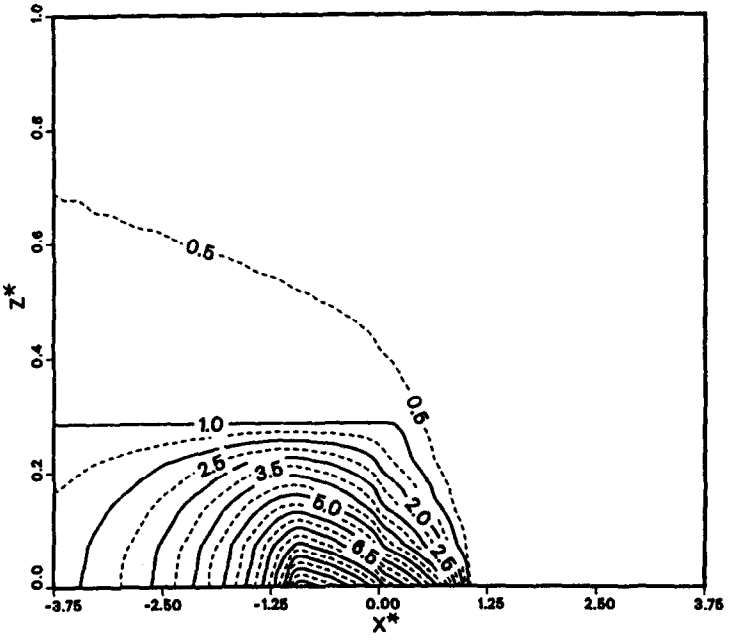

FIG. 9. Isotherms of the solution for $t = 0.1$ s at the X–X plane.

$T^* = (T-T_i)/(T_m-T_i)$ for $t = 0.1$ s along the X–X plane. Other parameters are $N_v = 1.2$, $N_Q = 60$, $St = 0.001$, $C_{sw} = 0.94$, $C_{lw} = 1.38$, $K_{lw} = K_{sw} = 0.65$, $\delta^* = 0.51$ and $h^* = 1.45$. The center of the heat source is located at $x = 0$. The solid line labelled 1.0 indicates the melting front at this time. After about 0.5 s, the steady-state condition is reached. Figure 10 shows the corresponding steady-state isotherms of the dimensionless temperature at the same plane. The melting front is also labelled 1.0.

Figure 11 shows the steady-state wall surface temperature along the X–X plane with different Stefan numbers, $St = c_s(T_m-T_i)/H$. Also shown in the figure is a pure wall (without PCM) having the same weight per unit surface area as that of the wall–PCM module. As can be seen, the reduction of the peak wall temperature is significant. In the figure, $\delta_m^* = \delta_m/R_h$ is the dimensionless maximum melting front depth, where δ_m is the maximum melting front depth from the wall surface corresponding to the steady state.

The dimensionless wall thickness δ^* has a significant influence on the temperature distribution. With a smaller δ^* the reduction of the peak wall temperature is more evident, as shown in Fig. 12.

Like the moving heat source problem without phase change, when N_v is small enough and N_Q is large enough the dimensionless temperature will become high, as shown in Fig. 13. The case with $N_v = 0.3$ and $N_Q = 60$ has a peak wall temperature almost four times as high as that with $N_v = 2.4$ and $N_Q = 30$. In this situation, perhaps one has to resort to another alternative.

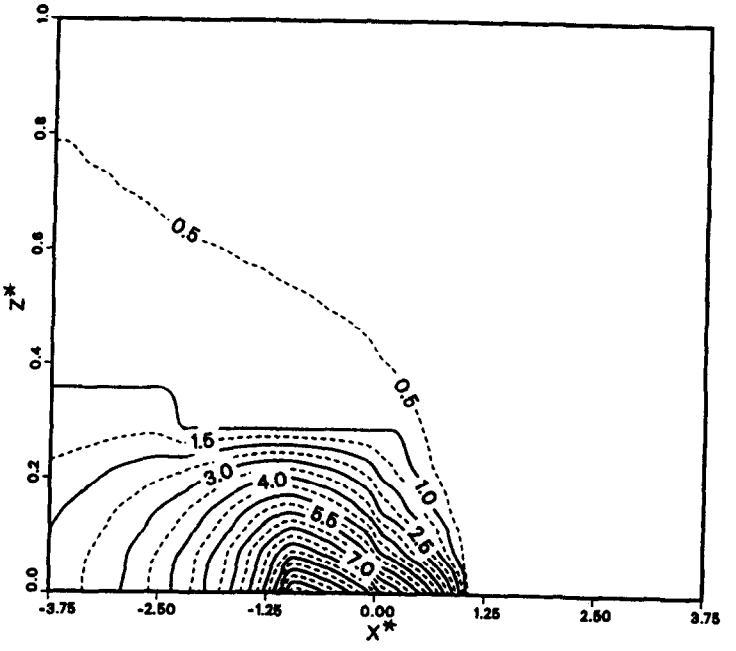

FIG. 10. Steady-state isotherms of the solution at the X–X plane.

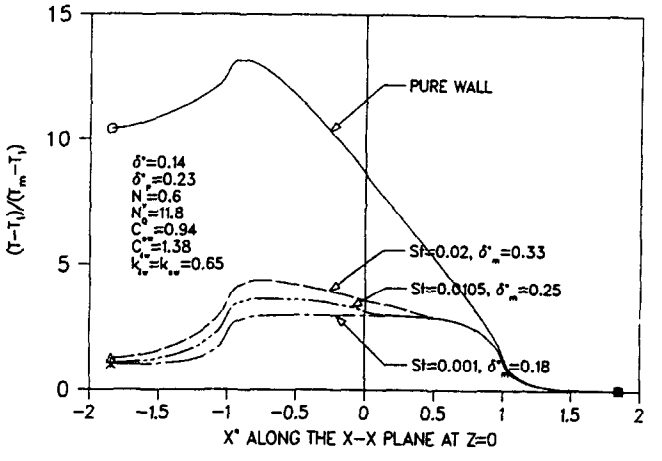

FIG. 11. Steady-state temperature profiles with different St.

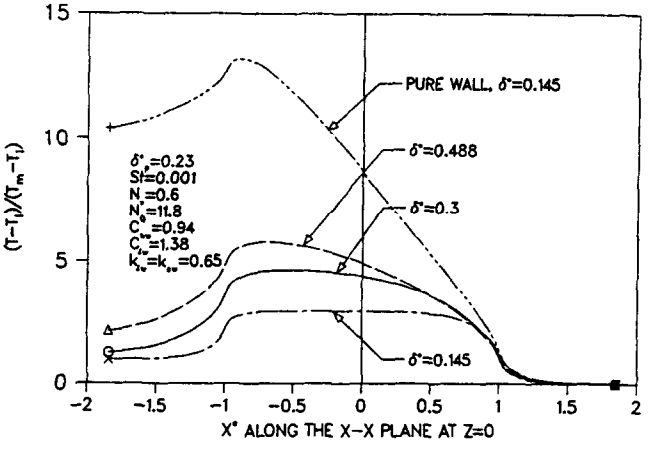

FIG. 12. Steady-state temperature profiles with different δ^*.

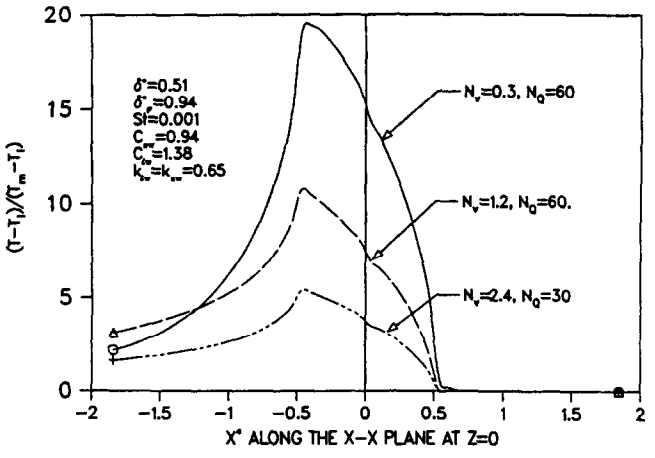

FIG. 13. Steady-state temperature profiles with different N_v and N_Q.

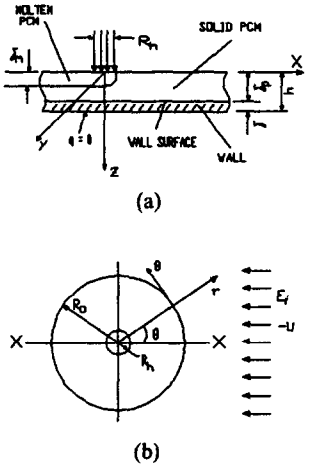

FIG. 14. Pictorial description of the computational domain for the PCM–wall module: (a) side view; (b) top view.

(3) *Moving heat source with PCM coated on the surface*

The configuration of this technology of protecting the surface is illustrated in Fig. 14. The numerical procedure is similar to that with PCM beneath the wall. The calculation is conducted with three different Stefan numbers and the results are shown in Fig. 15. The liquid phase in the numerical domain is assumed not to be blown away in this situation. Also shown in the figure is the temperature distribution of a pure plane (without PCM) having the same weight per unit surface area as that of the PCM–wall module indicated in Fig. 14. It is evident that the dimensionless temperature of the wall surface with PCM coated on it has no way to exceed one, which means that the wall surface temperature will be less than T_m, provided that the maximum melting front depth is less than the thickness of the PCM coat on the surface.

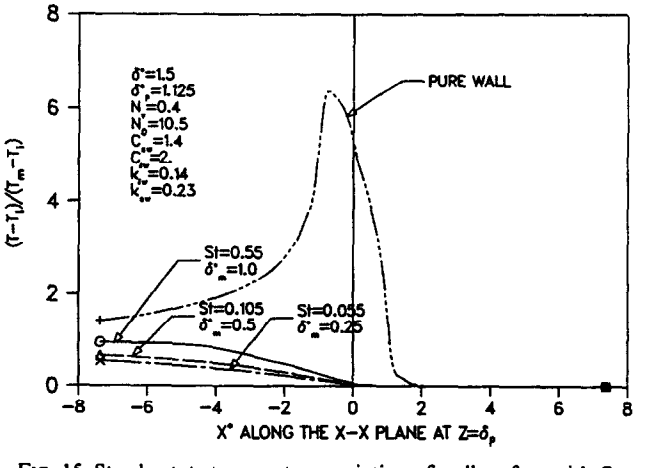

FIG. 15. Steady-state temperature variation of wall surface with St.

CONCLUSIONS AND REMARKS

If a wall surface is subject to an intense moving heat flux, and with a large N_Q and a small N_r, the surface is prone to be burned out unless some measure is taken to protect it. The use of PCM proves to be a good means of protecting the surface in this respect. One way to protect the surface is to put the PCM underneath the wall. This method is more efficient with smaller St and δ^*. With N_Q increasing and N_r decreasing further, the method of coating the PCM on the surface is needed to protect the surface. In this situation, the wall surface temperature will be less than T_m provided that the maximum melting depth is less than the thickness of the PCM coat on the surface. It should be pointed out that both methods have advantages and disadvantages. Even if the method of putting the PCM underneath the wall is less efficient when N_Q and N_r are beyond some limits, it is ready to be used again and puts no restrictions on the wall surface. In these cases a trade-off will be reached when selecting the protective technology.

Acknowledgement—Funding for this work was provided by the Thermal Energy Group of the Aero Propulsion Laboratory of the U.S. Air Force under contract F33615-88-C-2820.

REFERENCES

1. W. M. Kays and M. E. Crawford, *Convective Heat and Mass Transfer* (2nd Edn). McGraw-Hill, New York (1980).
2. M. Okada, Analysis of heat transfer during melting from a vertical wall, *Int. J. Heat Mass Transfer* **27**, 2057–2066 (1984).
3. C. J. Ho and S. Chen, Numerical simulation of melting of ice around a horizontal cylinder, *Int. J. Heat Mass Transfer* **29**, 1359–1368 (1986).
4. N. Shamsundar and E. M. Sparrow, Analysis of multidimensional conduction phase change via the enthalpy model, *ASME J. Heat Transfer* **97**, 333–340 (1975).
5. V. R. Voller and M. Cross, Estimating the solidification/melting times of cylindrically symmetric regions, *Int. J. Heat Mass Transfer* **24**, 1457–1462 (1981).
6. Y. Cao, A. Faghri and W. S. Chang, A numerical analysis of Stefan problems for generalized multi-dimensional phase-change structures using the enthalpy transforming model, *Int. J. Heat Mass Transfer* **32**, 1289–1298 (1989).
7. A. D. Solomon, M. D. Morris, J. Martin and M. Olszewski, The development of a simulation code for a latent heat thermal energy storage system in a space station, Technical Report ORNL-6213 (1986).
8. S. V. Patankar, *Numerical Heat Transfer and Fluid Flow*. McGraw-Hill, New York (1980).

PROTECTION VIS-A-VIS DE FLUX THERMIQUES LOCALISES, INTENSES ET MOBILES EN UTILISANT DES MATERIAUX A CHANGEMENT DE PHASE

Résumé—On examine plusieurs technologies pour protéger une paroi de son brûlage par une source de chaleur localisée, intense, mobile et on propose une solution selon laquelle un matériau à changement de phase (PCM) est placée juste dessous la paroi pour absorber le grand flux de chaleur. Le problème de fusion tridimensionnelle est réduit et modélisé par un schéma enthalpique nouveau. Les résultats numériques montrent que la solution proposée réduit significativement le pic de la température pariétale. La méthode de dépôt du PCM sur la paroi est aussi employée pour maintenir la température de surface au dessous de la température de fusion du PCM.

THERMISCHER SCHUTZ GEGEN INTENSIVE, ÖRTLICH BEGRENZTE, WANDERNDE WÄRMESTRÖME DURCH VERWENDUNG VON PHASEN-WECHSEL-MATERIALIEN

Zusammenfassung—Es wurden zahlreiche Methoden zur Vermeidung von "Burn-Out-Effekten" an Heizwänden durch intensive, örtlich begrenzte, wandernde Wärmequellen untersucht. Es wird eine Lösung für das Problem vorgeschlagen, bei der ein Phasen-Wechsel-Material (PCM) unterhalb der Wandoberfläche angebracht wird, um den großen Wärmestrom zu absorbieren. Das dreidimensionale Schmelz-Problem wird in dimensionsloser Form durch ein neuartiges Enthalpie-Transformations-Verfahren beschrieben. Die numerischen Ergebnisse zeigen, daß die vorgeschlagene Lösung die maximale Wandtemperatur signifikant reduziert. Mit einer weiteren angewandten Methode, bei der die Wandoberfläche mit dem PCM beschichtet wird, kann die Oberflächentemperatur unterhalb der Schmelztemperatur des PCM's gehalten werden.

ТЕПЛОЗАЩИТА ОТ ИНТЕНСИВНЫХ ЛОКАЛИЗОВАННЫХ ДВИЖУЩИХСЯ ИСТОЧНИКОВ ТЕПЛА С ИСПОЛЬЗОВАНИЕМ МАТЕРИАЛОВ С ФАЗОВЫМ ПЕРЕХОДОМ

Аннотация—Проведен обзор различных технологий защиты стенки от сгорания при воздействии интенсивного локализованного движущегося источника тепла, и предложено решение данной задачи, в котором материал с фазовым переходом (МФП) помещается под стенку для поглощения теплового потока большой величины. Трехмерная задача плавления приводится к безразмерному виду и моделируется по новой схеме превращения энтальпии. Численные результаты показывают, что предложенное решение значительно уменьшает максимальную температуру стенки. Используется также способ нанесения МФП на поверхность стенки, позволяющий поддерживать температуру поверхности ниже точки плавления МФП.